ELSEVIER

Journal of Alloys and Compounds 408–412 (2006) 1132–1135

Journal of ALLOYS AND COMPOUNDS

www.elsevier.com/locate/jallcom

Redox behavior of CeO_2–ZrO_2–Bi_2O_3 and CeO_2–ZrO_2–Y_2O_3 solid solutions at moderate temperatures

K. Minami [a], T. Masui [a], N. Imanaka [a,*], L. Dai [b], B. Pacaud [b]

[a] *Department of Applied Chemistry, Faculty of Engineering and Handai Frontier Research Center, Osaka University, 2-1 Yamadaoka, Suita, Osaka 565-0871, Japan*

[b] *Research and Development Department, Anan Kasei Co. Ltd., 210-51 Ohgata-cho, Anan, Tokushima 774-0022, Japan*

Received 30 July 2004; received in revised form 15 December 2004; accepted 15 December 2004
Available online 14 June 2005

Abstract

A CeO_2–ZrO_2–Bi_2O_3 solid solution for a promoter in the automotive three-way catalysts was synthesized by the calcination of the co-precipitated oxalate powder at 1273 K. Compared with the conventional binary CeO_2–ZrO_2 and ternary CeO_2–ZrO_2–Y_2O_3 solid solutions, the present CeO_2–ZrO_2–Bi_2O_3 solid solution can release and store oxygen efficiently at lower temperatures (600 K). The reason for such a behavior is attributed to the formation of oxygen vacancies to enhance the oxide anion mobility by substituting Ce^{4+} or Zr^{4+} site with Bi^{3+}, and also to the simultaneous reduction of Ce^{4+} and Bi^{3+} in the CeO_2–ZrO_2–Bi_2O_3 solid solution.

Keywords: Automotive exhaust catalyst; Oxygen storage capacity; Promoter; Ceria–zirconia; Bismuth oxide

1. Introduction

The exhaust gases from gasoline vehicles, especially CO, NO_x and hydrocarbons (HCs), have caused several environmental problems and the automotive three-way catalysts are widely used to eliminate these toxic compounds [1–4]. In the three-way catalysts, CeO_2 plays a significant role in adjusting the air/fuel ratio where the catalysts can purify the toxic gases in the converters effectively [1], because CeO_2 acts as an oxygen buffer by storing/releasing oxygen due to the Ce^{3+} and Ce^{4+} redox couple [5]. Higher oxygen storage/release capacity (OSC) of the catalyst becomes higher conversion efficiency is generally observed.

However, CeO_2 has a poor thermal stability and is known to be easily sintered at high temperatures [6]. In order to increase the OSC and the thermal stability, ZrO_2 is dissolved into the lattice of CeO_2 [7,8]. Although these properties have been improved by the ZrO_2 addition, the OSC at low temperatures is not enough to meet the regulations of the automotive exhaust gases, which become stricter year by year. Therefore, it has been required to enhance the redox activities of the catalysts at low temperatures.

Furthermore, removal of the particulate matters released from diesel vehicles has been attracted in recent years considerably, because it is not only useless but also harmful for human beings and environment. In addition, stringent regulations on the emission of the particulate matters have also been established. Therefore, it has been required to develop novel catalysts, which can adapt to the regulations, which become stricter year by year.

As a work on this line, we have prepared a CeO_2–ZrO_2–Bi_2O_3 solid solution not only to improve the OSC but also to promote combustion of soot included in the particulate matters at low temperatures. The reasons for choosing Bi_2O_3 as the third component are as follows: (1) Bi_2O_3 in itself has high oxide anion conductivity, (2) Bi_2O_3 is easily reduced to release oxygen [9–11] and (3) Bi^{3+} has lower valence (trivalent) than Ce^{4+} and Zr^{4+} (tetravalent), which promotes the formation of oxygen vacancies. In order to elucidate the effectiveness of the Bi_2O_3 doping, a CeO_2–ZrO_2–Y_2O_3 solid

* Corresponding author. Tel.: +81 6 6879 7352; fax: +81 6 6879 7354.
E-mail address: imanaka@chem.eng.osaka-u.ac.jp (N. Imanaka).

0925-8388/$ – see front matter © 2005 Elsevier B.V. All rights reserved.
doi:10.1016/j.jallcom.2004.12.141

solution was also synthesized to compare the redox property with that of the CeO_2–ZrO_2–Bi_2O_3 sample.

2. Experimental

The CeO_2–ZrO_2–M_2O_3 (M = Bi or Y) samples were prepared by the co-precipitation method. In these samples, the molar ratio of Ce:Zr:M (M = Bi or Y) was adjusted to be 64:16:20. A mixed solution of 1 mol L^{-1} $Ce(NO_3)_3$, 1 mol L^{-1} $ZrO(NO_3)_2$ and 0.1 mol L^{-1} $Bi(NO_3)_3$ aqueous solutions was dropped into a 0.5 mol L^{-1} oxalic acid aqueous solution with stirring. After dropping the mixed solution, 3 mol L^{-1} ammonia water was added into the mixed solution until the pH value of the solution became 3.2. After stirring overnight, the precipitated oxalate was filtered off and then dried at 353 K overnight. The dried powder was ground in an agate mortar and was calcined at 1273 K in air for 1 h. In the case of the CeO_2–ZrO_2–Y_2O_3 sample, a 1 mol L^{-1} $Y(NO_3)_3$ aqueous solution was used instead of $Bi(NO_3)_3$. In addition, the binary CeO_2–ZrO_2 solid solution (Ce:Zr = 80:20) was also prepared for comparison.

The samples obtained were characterized by X-ray powder diffraction (XRD, Rigaku MultiFlex), X-ray fluorescent analysis (Rigaku ZSX100e) and Raman spectroscopy (Kaiser Optical Systems, Inc. Holoprobe). Reduction behavior was determined by temperature programmed reduction (TPR) in a pure hydrogen flow (80 mL min^{-1}) at a heating rate of 5 K min^{-1}. Oxygen storage capacity was measured after the TPR measurement by a pulse method at 700 K. The combustion temperature of soot (CABOT CAS No.1333-86-4) was evaluated by thermogravimetric (TG) analysis using the samples containing 2 wt% of soot in a flow of air (20 mL min^{-1}).

3. Results and discussion

The sample composition determined by the X-ray fluorescent analysis was mostly in agreement with the theoretical composition as summarized in Table 1. Fig. 1 shows the XRD patterns of the samples. All of the profiles were attributed to the cubic fluorite structure. Because the peaks of $Ce_{0.64}Zr_{0.16}Bi_{0.20}O_{1.9}$ and $Ce_{0.61}Zr_{0.17}Y_{0.22}O_{1.89}$ shifted to the higher angle compared with $Ce_{0.86}Zr_{0.14}O_{2.0}$, it is considered that Bi^{3+} or Y^{3+} dissolves into the CeO_2–ZrO_2 lattice to form solid solutions.

It seems that the XRD patterns of the $Ce_{0.86}Zr_{0.14}O_{2.0}$, the $Ce_{0.64}Zr_{0.16}Bi_{0.20}O_{1.9}$ and the $Ce_{0.61}Zr_{0.17}Y_{0.22}O_{1.89}$ samples are similar. However, a clear difference was observed

Table 1
Composition of the samples

Theoretical composition	Analyzed composition
$Ce_{0.80}Zr_{0.20}O_{2.0}$	$Ce_{0.86}Zr_{0.14}O_{2.0}$
$Ce_{0.64}Zr_{0.16}Bi_{0.20}O_{1.9}$	$Ce_{0.64}Zr_{0.16}Bi_{0.20}O_{1.9}$
$Ce_{0.64}Zr_{0.16}Y_{0.20}O_{1.9}$	$Ce_{0.61}Zr_{0.17}Y_{0.22}O_{1.89}$

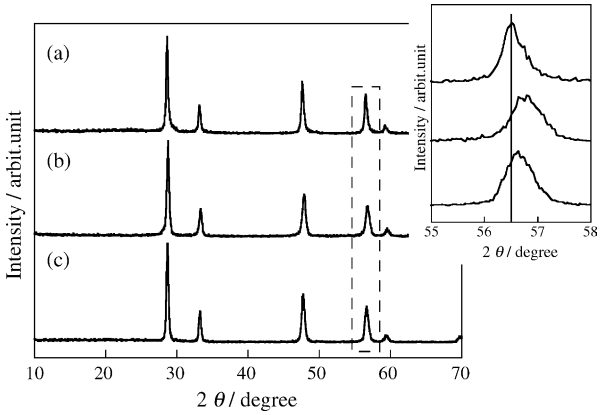

Fig. 1. XRD patterns of the samples: (a) $Ce_{0.86}Zr_{0.14}O_{2.0}$, (b) $Ce_{0.64}Zr_{0.16}Bi_{0.20}O_{1.9}$ and (c) $Ce_{0.61}Zr_{0.17}Y_{0.22}O_{1.89}$.

in their Raman spectra as depicted in Fig. 2. In the binary $Ce_{0.86}Zr_{0.14}O_{2.0}$ sample, only a single F_{2g} mode of the cubic fluorite structure was observed at 470 cm^{-1} [12]. On the other hand, some minor peaks were additionally observed at 315 and 573 cm^{-1} in the $Ce_{0.64}Zr_{0.16}Bi_{0.20}O_{1.9}$ sample and only one additional peak was observed at 562 cm^{-1} in the $Ce_{0.61}Zr_{0.17}Y_{0.22}O_{1.89}$ sample in addition to the main strong band around 470 cm^{-1}. Such a spectral feature is attributed to the formation of t'' phase, which is a kind of tetragonal structure containing oxygen displacement [13]. Since the peak at 315 cm^{-1} was not observed in $Ce_{0.61}Zr_{0.17}Y_{0.22}O_{1.89}$, it is considered that the displacement of the oxide anions from the ideal tetrahedral sites is relatively smaller than that of $Ce_{0.64}Zr_{0.16}Bi_{0.20}O_{1.9}$. Therefore, it is expected that the reduction temperature of the $Ce_{0.64}Zr_{0.16}Bi_{0.20}O_{1.9}$ sample is much lower than that of $Ce_{0.61}Zr_{0.17}Y_{0.22}O_{1.89}$, although

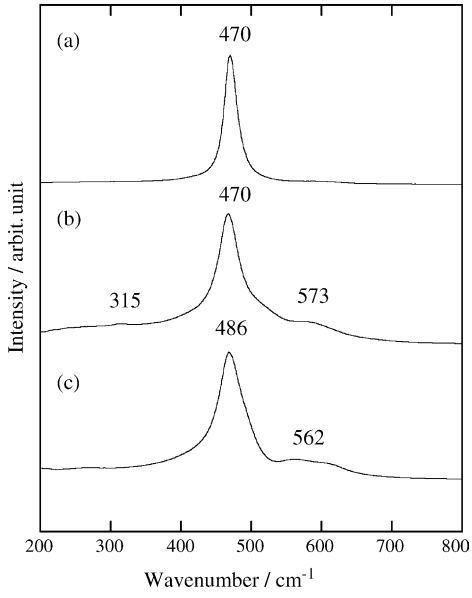

Fig. 2. Raman spectra of the samples: (a) $Ce_{0.86}Zr_{0.14}O_{2.0}$, (b) $Ce_{0.64}Zr_{0.16}Bi_{0.20}O_{1.9}$ and (c) $Ce_{0.61}Zr_{0.17}Y_{0.22}O_{1.89}$.

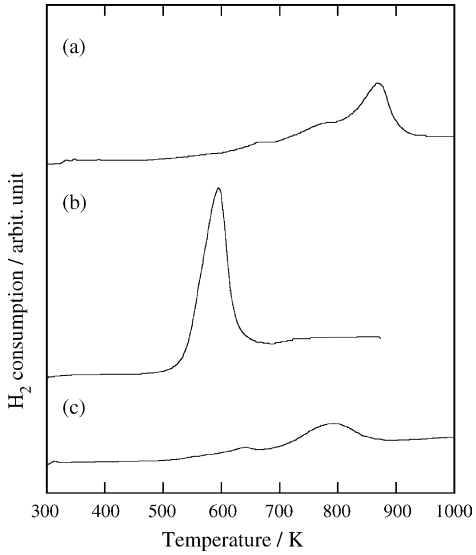

Fig. 3. TPR profiles of the samples: (a) $Ce_{0.86}Zr_{0.14}O_{2.0}$, (b) $Ce_{0.64}Zr_{0.16}Bi_{0.20}O_{1.9}$ and (c) $Ce_{0.61}Zr_{0.17}Y_{0.22}O_{1.89}$.

both reduction temperatures should become lower than that of the binary $Ce_{0.86}Zr_{0.14}O_{2.0}$ sample.

TPR profiles of the $Ce_{0.86}Zr_{0.14}O_{2.0}$, the $Ce_{0.64}Zr_{0.16}Bi_{0.20}O_{1.9}$ and the $Ce_{0.61}Zr_{0.17}Y_{0.22}O_{1.89}$ samples are illustrated in Fig. 3. The $Ce_{0.64}Zr_{0.16}Bi_{0.20}O_{1.9}$ solid solution released oxygen at the lowest temperature (590 K) among them and it was 300 K lower than that of the $Ce_{0.86}Zr_{0.14}O_{2.0}$ sample due to the formation of the t'' phase accompanying with the production of the oxygen vacancies. However, the temperature at which the $Ce_{0.61}Zr_{0.17}Y_{0.22}O_{1.89}$ sample released oxygen was not as low as 590 K, although the $Ce_{0.61}Zr_{0.17}Y_{0.22}O_{1.89}$ sample also has the t'' structure and oxygen vacancies exist in the lattice. The reason for this different behavior is attributable to the reduction of Bi^{3+} in addition to the different extent of the oxygen displacement. In $Ce_{0.64}Zr_{0.16}Bi_{0.20}O_{1.9}$, both Ce^{4+} and Bi^{3+} are reduced simultaneously, while only Ce^{4+} is reduced in $Ce_{0.61}Zr_{0.17}Y_{0.22}O_{1.89}$. As a result, the reduction temperature of the former becomes much lower than that of the latter. In fact, the OSC value of $Ce_{0.64}Zr_{0.16}Bi_{0.20}O_{1.9}$ is twice as high as that of $Ce_{0.86}Zr_{0.14}O_{2.0}$ as summarized in Table 2. On the other hand, the OSC value of $Ce_{0.61}Zr_{0.17}Y_{0.22}O_{1.89}$ was a little smaller than that of $Ce_{0.86}Zr_{0.14}O_{2.0}$, because the amount of Ce^{4+} ion in $Ce_{0.61}Zr_{0.17}Y_{0.22}O_{1.89}$ decreases by the substitution of Ce^{4+} site with Y^{3+}.

The $Ce_{0.64}Zr_{0.16}Bi_{0.20}O_{1.9}$ material we proposed in the present study utilizes one of the unique characteristics of

Table 2
Oxygen storage capacity (OSC) of the samples

Composition	OSC (μmol O_2 g^{-1})
$Ce_{0.80}Zr_{0.20}O_{2.0}$	482
$Ce_{0.64}Zr_{0.16}Bi_{0.20}O_{1.9}$	1036
$Ce_{0.61}Zr_{0.17}Y_{0.22}O_{1.89}$	361

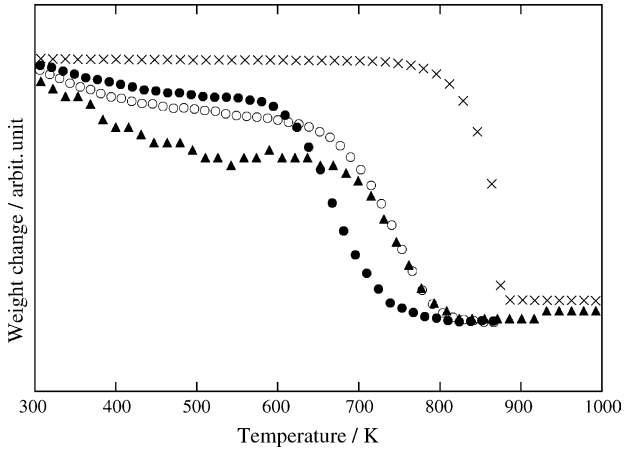

Fig. 4. TG analysis for the evaluation of soot combustion temperature; $Ce_{0.86}Zr_{0.14}O_{2.0}$ + 2 wt% soot (○), $Ce_{0.64}Zr_{0.16}Bi_{0.20}O_{1.9}$ + 2 wt% soot (●), $Ce_{0.61}Zr_{0.17}Y_{0.22}O_{1.89}$ + 2 wt% soot (▲) and soot only (×).

Bi_2O_3 that it is reduced to metallic Bi easily, and a slight phase separation of Bi_2O_3 was observed in the reoxidized samples after the TPR measurement up to 1273 K. However, the TPR profiles can be reproducible when the reduction was carried out up to 873 K, and no phase separation was observed. Therefore, we believe that these materials could be applied to alternative catalyst components, especially for motorcycles in which the catalysts have to work at lower temperatures than those in automobiles.

Fig. 4 shows the TG analysis for soot combustion in these catalysts. The combustion temperature became lowest when the soot was mixed with the $Ce_{0.64}Zr_{0.16}Bi_{0.20}O_{1.9}$ catalyst. However, the soot combustion temperature for $Ce_{0.61}Zr_{0.17}Y_{0.22}O_{1.89}$ was almost the same as that of $Ce_{0.86}Zr_{0.14}O_{2.0}$. These results correspond to their reduction temperatures, because active oxygen released from $Ce_{0.64}Zr_{0.16}Bi_{0.20}O_{1.9}$ bulk at low temperatures promotes the soot combustion. Consequently, it can be concluded that low temperature reduction behavior is considerably effective to the low temperature combustion of soot.

4. Conclusions

Bismuth oxide was dissolved into the CeO_2–rO_2 lattice in order to synthesize a new solid solution, which can release and storage oxygen at low temperatures. The $Ce_{0.64}Zr_{0.16}Bi_{0.20}O_{1.9}$ sample obtained can release oxygen at the temperature lower than 300 K compared with the case for the conventional $Ce_{0.86}Zr_{0.14}O_{2.0}$. However, such a behavior was not observed when Y_2O_3 is dissolved into CeO_2–ZrO_2, clearly indicating the superiority of the bismuth doping. The reason for such effectiveness is attributed to the synergistic effect of the easy reduction of Bi_2O_3 in itself and the formation of the t'' phase by the Bi doping, which accelerates oxide ion migration at low temperatures.

Acknowledgements

The authors sincerely thank Dr. Kuniaki Murase and Prof. Yasuhiro Awakura (Kyoto University) for their assistance with the Raman spectra measurements. This work was supported by the Industrial Technology Research Grant Program in 02 (Project No. 02A27004c) from the New Energy and Industrial Technology Development Organization (NEDO) based on funds provided by the Ministry of Economy, Trade and Industry, Japan (METI).

References

[1] J. Kašpar, P. Fornasiero, M. Graziani, Catal. Today 50 (1999) 285.
[2] R.J. Farrauto, R.M. Heck, Catal. Today 51 (1999) 351.
[3] M. Shelef, R.W. McCabe, Catal. Today 62 (2000) 35.
[4] J.T. Kummer, J. Phys. Chem. 90 (1986) 4747.
[5] H.C. Yao, Y.F. Yao, J. Catal. 86 (1984) 254.
[6] J. Kašpar, P. Fornasiero, N. Hickey, Catal. Today 77 (2003) 419.
[7] J.R. González-Velasco, M.A. Gutiérrez-Ortiz, J.-L. Marc, J.A. Botas, M.P. González-Macros, G. Blanchard, Appl. Catal. B Environ. 22 (1999) 167.
[8] P. Fornasiero, G. Balducci, R. Di Monte, J. Kašpar, V. Sergo, G. Gubitosa, A. Ferrero, M.J. Graziani, J. Catal. 164 (1996) 173.
[9] T. Takahashi, H. Iwahara, T. Esaka, J. Electrochem. Soc. 124 (1977) 1563.
[10] P. Shuk, H.-D. Wiemhöfer, U. Guth, W. Göpel, M. Greenblatt, Solid State Ionics 89 (1996) 179.
[11] S. Dikmen, P. Shuk, M. Greenblatt, Solid State Ionics 112 (1998) 299.
[12] V.G. Keramidas, W.B. White, J. Am. Ceram. Soc. 57 (1974) 22.
[13] M. Yashima, H. Arashi, M. Kakihana, M. Yoshimura, J. Am. Ceram. Soc. 77 (1994) 1067.